Springer

KSME

Journal of Mechanical Science and Technology 26 (5) (2012) 1633~1641
www.springerlink.com/content/1738-494x
DOI 10.1007/s12206-012-0324-8

Effects of gas and particle emissions on wall radiative heat flux in oxy-fuel combustion †

Sanghyun Park[1], Jungeun A. Kim[1], Changkook Ryu[1,*], Won Yang[2], Young Ju Kim[3] and Sangil Seo[3]

[1]*School of Mechanical Engineering, Sungkyunkwan University, Suwon, 440-746, Korea*
[2]*Energy System R&D Group, Korea Institute of Industrial Technology, Cheonan, 330-825, Korea*
[3]*Green Energy Lab. Korea Electric Power Research Institute, Daejeon, 305-380, Korea*

(Manuscript Received September 1, 2011; Revised January 15, 2012; Accepted February 1, 2012)

Abstract

Oxy-fuel combustion exhibits combustion and heat transfer characteristics different from air-fuel combustion due to high concentrations of CO_2 and H_2O. This study evaluated the effect of gas and particle emissions on radiative heat transfer in oxy-fuel combustion of coal. For a hexahedral furnace, prescribed gas compositions based on combustion calculation were used to simplify the combustion reactions. The values of radiative heat fluxes (q_{rad}) were compared for different combustion modes, flue gas recirculation (FGR) methods, particle concentrations, furnace sizes and O_2 concentrations in the oxidizer. The radiation was calculated by the discrete ordinate method with gaseous emission predicted by the weighted sum of gray gases models (WSGGMs). The results showed that employing an optimized WSGGM is essential for the accurate prediction of q_{rad} in oxy-fuel combustion for gaseous fuels. The conventional WSGGM showed large errors for larger furnace volumes or under dry FGR conditions. With higher particle concentrations such as in pulverized coal combustion, however, q_{rad} was dominated by emission of particles. The effect of gas emissivity was not critical in the furnace with a mean beam length of 8.3m. Oxy-fuel combustion with wet FGR had higher q_{rad} than dry FGR. The O_2 concentration in the oxidizer was a key parameter for oxy-fuel combustion since increasing its value linearly increased q_{rad}.

Keywords: Gas emissivity; Oxy-coal combustion; Particle emission; Radiation; Weighted sum of gray gases model

1. Introduction

Oxy-fuel combustion is one of the main technologies for CO_2 capture and storage (CCS) at fossil fuel fired power plants [1]. In order to supply O_2 for oxy-fuel combustion, N_2 is removed from air using an air separation unit (ASU). The remaining gases which comprise approximately 95 vol.% O_2 and impurities, such as Ar, are used as oxidizers. In order to prevent furnaces from reaching excessively high temperatures, flue gas containing mainly CO_2 and H_2O is recirculated and subsequently mixed with the oxidizer. After heat recovery and gas cleaning, the flue gas is processed to condense H_2O. Then, the high purity CO_2 is compressed and liquefied for carbon storage. Flue gas recirculation (FGR) could be wet or dry, depending on whether the flue gas is taken before or after the H_2O removal.

The oxy-fuel combustion concept can be simplified to combustion using surrogate air in which N_2 is replaced with CO_2. However, the combustion characteristics in oxy-fuel combustion differ from that with air due to significant differences in the physical properties of CO_2 and N_2 [1, 2]. CO_2 has a lower specific volume than N_2, which influences swirl, flame shape and gas volume [3]. The lower specific volume also leads to higher volumetric heat capacity that directly affects the temperature distribution. In order to maintain sufficiently high temperatures, overall O_2 concentrations of 25-30 vol.% in the oxidizer are being considered for oxy-fuel combustion [4]. Unlike the inert N_2, CO_2 also reacts with char through the endothermic Boudouard reaction ($C(s)+CO_2 \rightarrow 2CO$), which may either accelerate the char burn-out or decelerate by lowering the particle temperature [5]. The amount of NOx per fuel throughput is reduced during oxy-fuel combustion mainly due to the low concentration of N_2 [1, 6-7], but significant increases in the SO_3 concentration are of a concern for gas cleaning [2, 8].

In regards to the performance of an oxy-fuel furnace, another crucial difference in the properties of gases is that CO_2 participates in radiation. With high partial pressures of CO_2

*Corresponding author. Tel.: +82 31 299 4841, Fax.: +82 31 290 5889
E-mail address: cryu@me.skku.ac.kr
† Recommended by Associate Editor Oh Chae Kwon.

and H_2O which sums up to almost 1 atm, gaseous emission under oxy-fuel combustion is stronger than that of flue gases in air-fuel combustion [9, 10].

Coal is currently the primary target for the application of oxy-fuel combustion. Since coal has the highest carbon content of common fossil fuels, the impact of carbon capture can be maximized. Furthermore, coal is also the main fuel used at large power plants. During combustion of pulverized coal, one important factor influencing radiation is the emission of particles such as coal, char and ash together with soot. The high concentration of particles contributes to q_{rad} on the wall to a degree much larger than gases [11]. Thus, some studies have argued that the difference in the gas emission characteristics is not critical during oxy-coal combustion [12]. Many experimental studies are being carried out in order to understand the flame, temperature and heat flux characteristics of oxy-coal combustion in various scales of test facilities. However, care must be taken when interpreting the results of radiation measurement or prediction, since q_{rad} greatly varies by many parameters including the furnace size, i.e., mean beam length (L_{mb}).

This study numerically assesses the relative importance of gas and particle emissions for radiation during air- and oxy-fuel combustion. Numerical simulations were carried out to investigate q_{rad} on the wall using the discrete ordinate method with three different WSGGMs in a hexahedral furnace. Prescribed gas compositions based on combustion calculation were used to simplify the combustion and reactions in the simulations. The values of q_{rad} were compared for different combustion modes, particle concentrations, furnace sizes and O_2 concentrations in the oxidizer. The results were discussed for applications in CFD modeling, combustion experiments at small scales and the design of a full-scale boiler.

2. Radiation model

The design of suitable combustion systems requires profound understanding of combustion characteristics such as flame shape, temperature and wall heat flux. Computational fluid dynamics (CFD) is often used to evaluate the performance of combustion systems at the design stage. Edge et al. [13] provided a good review on the CFD models applied to oxy-coal combustion. Among various submodels required to predict combustion, radiation becomes a source term in energy conservation that determines the local gas temperature, heating rate of fuel particles and heat flux on the wall.

Including the effect of particles and ignoring other sources of scattering, the radiative transfer equation (RTE) at position $\vec{r}$ in the direction $\vec{s}$ becomes [14]

$$\nabla\cdot\left(I\,\vec{s}\right)+\left(\alpha+\alpha_p+\sigma_p\right)I\left(\vec{r},\vec{s}\right)= \alpha n^2\frac{\sigma T^4}{\pi}+E_p+\frac{\sigma_p}{4\pi}\int_0^{4\pi} I\left(\vec{r},\vec{s}'\right)\Phi\left(\vec{s},\vec{s}'\right)d\Omega' . \quad (1)$$

I : Radiation intensity, α : Absorption coefficient of gas
α_p : Absorption coefficient of particles
E_p : Emission of particles, σ_p : Scattering factor of particles
n : Refractive index, T : Temperature

The discrete ordinates (DO) method is often used for the prediction of radiation. In this method, the RTE is represented by a discrete set of equations for the average intensity over a finite number of ordinate directions.

Among various levels of models available for gas emissivity, the WSGGM proposed by Hottel and Sarofim [15] is often used for practical CFD applications. The model greatly simplifies the calculation to reduce the computational costs by evaluating the gas emissivity (ε) from the weighted sum of gray gases.

$$\varepsilon=\sum_{i=0}^{I} a_{\varepsilon,i}\left(T_g\right)\left(1-e^{-\kappa_i P L_{mb}}\right) \quad (2)$$

$a_{\varepsilon,i}$: Weighting factor
κ_i : Absorption coefficient of gray gas i
$P=P_w+P_c$ (atm), I : The number of gray gases
L_{mb} : Mean beam length (m)

The weighting factors ($a_{\varepsilon,i}$) are fitted into J-th order polynomials of gas temperature (T_g), and the coefficients are tabulated together with the absorption coefficient (κ_i) for each gray gas i.

$$a_{\varepsilon,i}=\sum_{j=0}^{J} c_{i,j}T_g^{\,j} \quad (3)$$

L_{mb} is approximated from the volume and surface area of a furnace with a correction coefficient of 0.9 [14], as shown below:

$$L_{mb}=0.9\frac{4V}{A} . \quad (4)$$

From the gas emissivity, the effective absorption coefficient for gases is calculated as

$$\alpha=-\frac{\ln\left(1-\varepsilon\right)}{L_{mb}} . \quad (5)$$

The WSGGM proposed by Smith et al. [16] is commonly used for combustion, but the coefficients of this model are valid up to 10 atm·m of $P\cdot L_{mb}$. Since (P_w+P_c) is almost 1 atm in oxy-coal combustion, the use of this model is inappropriate for large furnaces. Moreover, the coefficients are not well-defined for dry FGR conditions of which a typical P_w/P_c ratio is about 0.125. To overcome such limitations, two separate models optimized for oxy-fuel combustion have recently been proposed by Johansson et al. [9] and Yin et al. [10], respectively. Table 1 compares the key features of the three models.

Both the Johansson and Yin models consider 4 gray gases

Table 1. Main features of the three WSGGMs.

WSGGM	Smith et al. [16]	Yin et al. [10]	Johansson et al. [9]
Valid ranges	PL: 0.001 ~ 10 atm·m 600<T<2400K	PL: 0.001 ~ 60 atm·m 500<T<3000K	L: 0.01 ~ 60m, P=1 bar 500<T<2500K
Number of gray gases	3	4	4, 3
Coefficients available for $a_{\varepsilon,i}$ and k_i	1) $P_c \rightarrow 0$ atm 2) $P_w \rightarrow 0$ 3) P_w =1 4) P_w/P_c=1 5) P_w/P_c=2	1) $P_w \rightarrow 0$; $P_c \rightarrow 0$ atm, 2) P_w =0.1; P_c =0.1 3) P_w =0.3; P_c =0.1, 4) P_w/P_c=0.125; P_w+P_c=1 5) P_w/P_c=0.25; P_w+P_c=1, 6) P_w/P_c=0.5; P_w+P_c=1 7) P_w/P_c=0.75; P_w+P_c=1, 8) P_w/P_c=1.0; P_w+P_c=1 9) P_w/P_c=2.0; P_w+P_c=1, 10) P_w/P_c=4.0; P_w+P_c=1	1) P_w/P_c=0.125 atm 2) P_w/P_c=1.0
Other features		T/T_{ref} used for $a_{\varepsilon,i}$ (T_{ref}=1200K)	T/T_{ref} used for $a_{\varepsilon,i}$ (T_{ref}=1200K)

Table 2. Test parameters and input conditions.

Case	Oxy27W	Oxy27D	Air21
O_2 in the oxidizer	27%	27%	21%
Product gas	CO_2: 47.30% H_2O: 45.85% P_w+P_c=0.932 atm P_w/P_c=0.969	CO_2: 75.68% H_2O: 15.57% P_w+P_c=0.912 atm P_w/P_c=0.206	CO_2: 12.80% H_2O: 12.41% P_w+P_c=0.252atm P_w/P_c=0.969
T_{af} (K)	2038	1949	2076
Furnace size (L_{mb})	2m×2m×6m ~ 28m×28m×84m (L_{mb}: 1.66m~23.3m)		
Particle flow rate	i) 0 % of ash in the coal (gas only), ii) ash 50%, iii) ash 100%, iv) ash 100% + FC 10%, v) ash 100% + FC 30%, vi) ash 100% + FC 50%		
Wall condition	-Conducting wall: emissivity 0.7, thickness 20mm, conductivity 19.8 W/m·K -Outer membrane wall: T_{mw} 603.15K, h_{mw} 1000W/m^2·K		

with a use of T_{ref} for accuracy in the polynomial expression of weighting factors, but the Yin model provides detailed subsets of P_w/P_c ratio for $c_{i,j}$ and κ_i.

With the presence of particles, α_p, σ_p and E_p for particles are calculated, respectively, as [17]

$$\alpha_p = \lim_{V\to 0}\sum_{n=0}^{N}\varepsilon_{p,n}\frac{A_{p,n}}{V} \tag{6}$$

$$E_p = \lim_{V\to 0}\sum_{n=0}^{N}\varepsilon_{p,n}\frac{A_{p,n}}{V}\frac{\sigma T_{p,n}^4}{\pi} \tag{7}$$

$$\sigma_p = \lim_{V\to 0}\sum_{n=0}^{N}\left(1-f_{p,n}\right)\left(1-\varepsilon_{p,n}\right)\frac{A_{p,n}}{V}. \tag{8}$$

$\varepsilon_{p,n}$: Emissivity of n-th particle, $A_{p,n}$: Projected area
$f_{p,n}$: Scattering factor, N : Total number of particles

3. Numerical methods

3.1 Input conditions for heat transfer simulations

Table 2 summarizes the test conditions for the numerical simulations. Different gas compositions were considered that represented the combustion conditions of (i) oxy-fuel combustion with dry FGR and (ii) with wet FGR and (iii) air-fuel combustion. The detailed properties for the product gas were determined from combustion calculations assuming complete combustion. The reference fuel selected in this study was a sub-bituminous coal [18]. It had a moisture content of 20 wt.%, fixed carbon 35 wt.% and ash 10 wt.%. The combustible fraction of the coal consisted of C 52.5 wt.%, H 6.3 wt.%, O 11.2 wt.%. The lower heating value of the coal was 22.4 MJ/kg. The flow rate of O_2 in the oxidizer was determined for an excess air ratio of 17%. In the oxidizer stream from ASU, transparent gases such as N_2 and Ar are present as the impurities. These gases transparent in terms of radiation were simplified into N_2 in the calculations. In the oxy-fuel combustion, the reference value of O_2 concentration in the oxidizer was 27% and other parameters were varied.

By combustion calculations, the total partial pressure (P_w+P_c) of H_2O and CO_2 in the product gas were determined to be 0.252 atm for air-fuel combustion (Case Air21, P_w/P_c=0.969), 0.932 atm for oxy-fuel combustion with wet FGR (Case Oxy27W, P_w/P_c=0.969), and 0.912 atm for dry FGR (Case Oxy27D, P_w/P_c=0.206). The adiabatic flame temperature (T_{af}) was 2076, 2038 and 1949 K for the three cases, respectively. The dry FGR case has the lowest T_{af} since the specific heat of CO_2 is the highest among the product gas components.

The effect of furnace size for each combustion condition was also investigated for a furnace size ranging from 2 m × 2 m × 6 m to 28 m × 28 m × 84 m. The corresponding values of L_{mb} were 1.66 m to 23.3 m. The fuel throughput and corresponding flow rate of product gas were varied by fixing the volumetric heat release rate at 0.13 MW/m^3 [19]. For example, the fuel throughput for the furnace with 10 m×10 m×30 m was 17.36 kg/s, and the resultant flow rate of product gas was 147.02, 182.78 and 171.31 kg/s for Cases Oxy27W, Oxy27D and Air21, respectively. The volumetric flow rate corresponded to 105.91, 105.91 and 132.80 Nm^3/s, respectively.

In order to investigate the effect of particles during pulverized coal combustion, the particle flow rates were varied from 0 (i.e., gas only without particles), 50% and 100% of the ash in the fuel and then up to 50% of fixed carbon content (FC) added. The particle size distribution was assumed to have a Rosin-Rammler distribution between 1 to 50 μm with an average of 25 μm. The particle emissivity was 0.9.

Once the flow rate, composition and temperature (T_{af}) of the product gas were determined, it entered the bottom of the hexahedral furnace and escaped at the top in the simulations. The boundary condition of the side walls directly affects the wall heat flux in the furnace. The emissivity at the furnace inlet and outlet was set to zero in order to remove their effects on the heat flux on the side walls. For comparison purposes between simulation cases with different furnace sizes, the wall was assumed to be a membrane wall with a temperature of 603.15 K, convection coefficient 1000 W/m^2·K and emissivity 0.7. The wall temperature was the saturated value at a steam pressure of about 128 bar which is for the plant being considered for demonstration of oxy-coal combustion in Korea at 100MWe scale. The overall heat flux at the side walls could then be predicted by radiation and convection by the gas and particles, conduction through the wall and finally by convection of the water/steam in the membrane wall.

3.2 Methods for heat transfer simulation

For numerical simulations, the commercial code of FLUENT (version 6.3) was used. Radiation was predicted by the DO method with an angular discretization of 5 divisions and 3 pixels both in the polar and azimuthal directions. The three WSGGMs described in the previous section were programmed into the code using the feature of user-defined subroutines for calculation of the emissivity and absorption coefficient. Turbulence of the gas was considered using the realizable k-ε model.

The mesh for the furnace was determined from sensitivity tests. The number of cells selected was 58,320 which showed a deviation less than 0.2% from the average radiative heat flux with 583,200 cells for the oxy-coal combustion with dry FGR condition.

4. Results and discussion

4.1 Gas emissivity

Fig. 1 compares the gas emissivity calculated by WSGGMs at different combustion conditions for L_{mb} up to 23.3m. Similar curves have already been presented in Johansson et al. [9] and Yin et al. [10], but are illustrated here for comprehensiveness. As described previously, the model by Smith et al. exhibited larger errors when L_{mb} increased over 10m for Case Oxy27W (Fig. 1(a)). The errors became more severe at dry FGR conditions in Fig. 1(b). Since the coefficients in the Smith model were provided at P_w/P_c = 1 and $P_w \rightarrow 0$, the calculation at dry FGR condition (P_w/P_c ~0.206) had to refer to the coefficients for $P_w \rightarrow 0$. This caused the large errors. For the air-fuel combustion case shown in Fig. 1(c), the Smith and Yin models agreed well with each other while the Johansson model was slightly overpredicted.

4.2 Contours of radiative heat flux

Fig. 2 compares the contours of q_{rad} for different cases. The

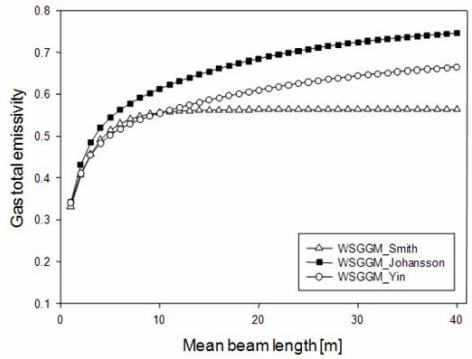

(a) Case Oxy27W

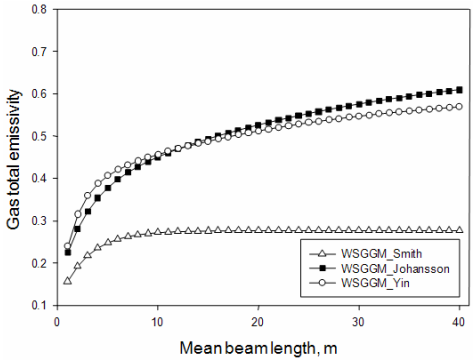

(b) Case Oxy27D

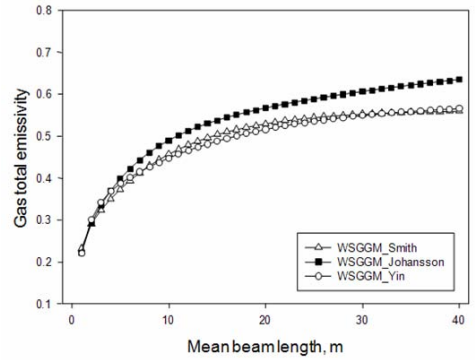

(c) Case Air21

Fig. 1. Comparison of total gas emissivity calculated by three WSGGMs for the mean beam length in oxy-fuel combustion with wet FGR (a), with dry FGR (b) and air-fuel combustion (c).

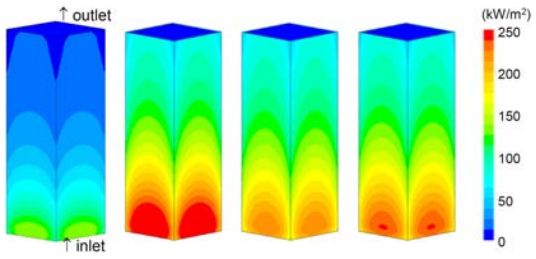

Fig. 2. Contours of wall radiative heat flux for cases without presence of particles: (a) Case Oxy27W with a furnace size of 2 m×2 m×6 m (L_{mb}=1.66 m); (b) Case Oxy27W, 10 m×10 m×30 m (L_{mb}=8.31 m); (c) Case Oxy27D, 10 m×10 m×30 m and (d) Case Air21, 10 m×10 m×30 m.

contours had parabolic profiles since the incident radiation concentrated at the center of the walls that had wider solid angles than the corners. As the gas temperature dropped due to radiative and convective heat loss, q_{rad} decreased in the upward direction. Larger furnaces had larger heat fluxes due to the increased L_{mb} as shown in Fig. 2(b). Dry FGR condition in Fig. 2(c) had lower heat flux. Since the profiles of heat flux on the wall were similar between cases, detailed results for different test parameters in further discussion are presented using the area-averaged q_{rad} on the wall. It is also noted that the contribution of convection was less than 3% of the total heat flux in all cases. Therefore, the discussion on the results is focused on the radiation.

4.3 Radiative heat flux without particles

Fig. 3 shows the area-averaged q_{rad} for different furnace sizes without presence of particles. The trends of heat flux well correlated with the gas emissivity shown in Fig. 1. Smaller furnaces had reduced values of q_{rad} due to smaller mean beam length and lower gas emissivity. The average q_{rad} of Case Oxy27W predicted by the Yin model for $L_{mb}=10$ m was about 161.9 kW/m^2 which was 14% and 7% larger than the values for Cases Oxy27D and Air21, respectively. In the largest furnace ($L_{mb}=23.3$ m), the value under wet FGR condition reached 240.5 kW/m^2.

When the gas emissivity was predicted by the Smith model, the dry FGR condition in Fig. 3(b) led to a large underestimation, which was only 67.8% of the value predicted by the Yin model at $L_{mb}=10$ m. Therefore, the use of appropriate WSGGM such as the Yin model was critical for the accurate prediction under oxy-fuel combustion of gaseous fuels with dry FGR. For the conventional air-combustion condition in Fig. 3(c), the three models predicted values very close to each other.

4.4 Effect of particle concentrations

Particle concentrations in a furnace become large for solid fuels, such as pulverized coal. Fig. 4 shows an example of particle concentration during coal combustion in a commercial 500 MWe-scale wall-firing furnace [20]. L_{mb} for this furnace was 13.0m. The particle concentration (Fig. 4(a)) widely varies from a few g/m^3 in the upper part of the furnace to over 50 g/m^3 in the burner region of the lower part. The volume averaged value in this furnace was 5.45 g/m^3. Therefore, its effect on radiation would be influenced strongly by the configuration of a furnace. Fig. 4(b) shows that q_{rad} in the commercial boiler was as high as 245 kW/m^2 in the burner region while the area-averaged value for the walls was 123.9 kW/m^2. Note that the approach in the present study assumed a uniform distribution of particles at a fixed flow rate. The volume-averaged concentration of particles was 4.05 g/m^3 at the particle flow rate of ash 100% and FC 10% for the furnace with $L_{mb}=8.31$ m in Case Oxy27W. The value was 3.21 g/m^3 in Case Air21, since this case had a larger volume flow rate with a lower gas density. In an actual furnace, the radiation by participation of particles would be stronger in the near-burner walls and weaker in the downstream of the gas flow as shown in Fig. 4.

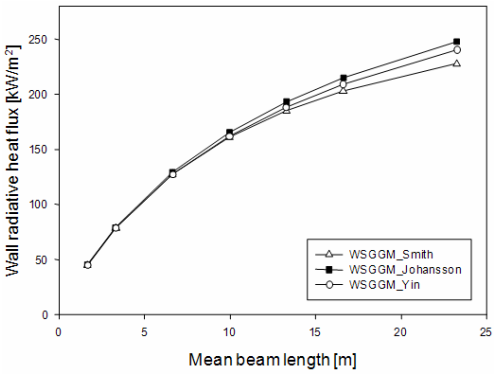

(a) Case Oxy27W

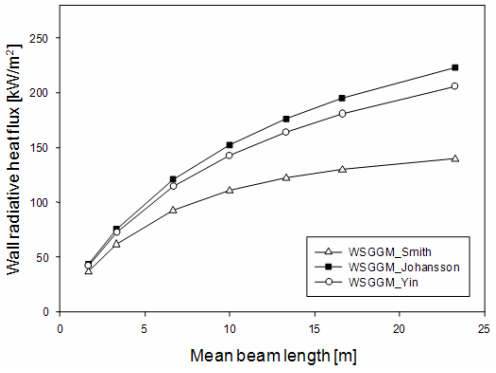

(b) Case Oxy27D

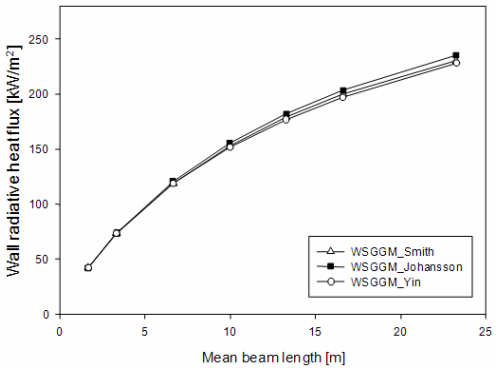

(c) Case Air21

Fig. 3. Effect of mean beam length on the average q_{rad} without particles (gas only) in oxy-fuel combustion with wet FGR (a) and with dry FGR (b) and air-fuel combustion (c).

Fig. 5 shows q_{rad} for three combustion conditions at $L_{mb}=1.66$m and 8.31m with various particle flow rates in the hexahedral furnace. The smaller furnace had q_{rad} gradually increased from 44.7 kW/m^2 to 48.5 kW/m^2 in Case Oxy27W, as the concentration and corresponding emissivity of particles increased (Fig. 5(a)). This case had higher values of q_{rad} but the differences between the cases remained only within 3

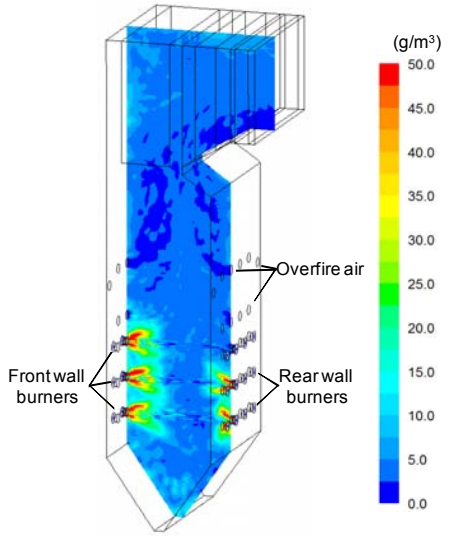

(a) Particle concentration (g/m^3)

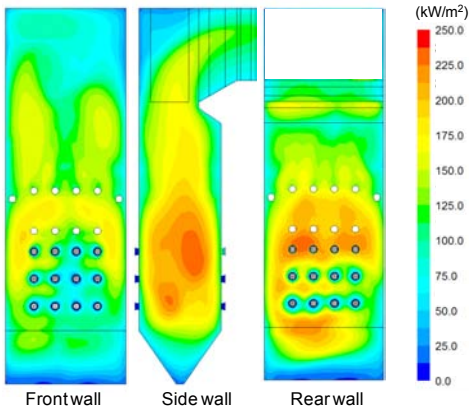

(b) Wall radiative heat flux (q_{rad}, kW/m^2)

Fig. 4. Indicative particle concentration and heat flux in a commercial 500MWe coal-fired furnace (L_{mb}=13.0 m).

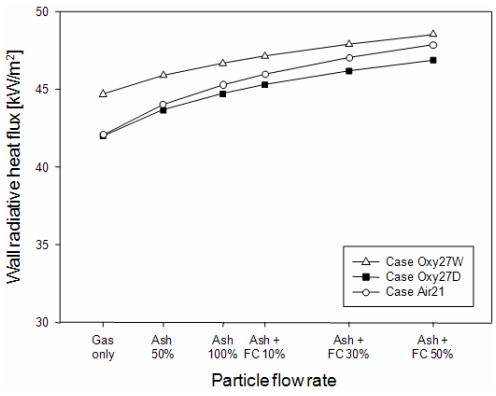

(a) L_{mb} = 1.66m

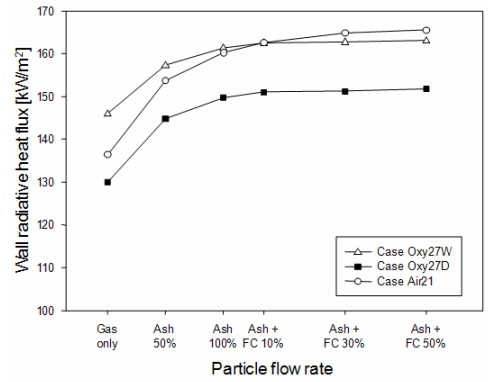

(b) L_{mb} = 8.31m

Fig. 5. Effect of particle concentration on the average q_{rad} for the three combustion cases (WSGGM: Yin model).

kW/m^2. For the larger furnace (Fig. 5(b)), the effect of particle concentration became more significant. When the particle flow rate was 100% of ash in the coal, the increase in q_{rad} was about 20-25 kW/m^2 in all the combustion cases. Further increase in particle concentration did not lead to a significant increase in q_{rad} since the radiation reached a saturation level. Between the combustion cases, Case Oxy27D case had the lowest values of q_{rad} due to the lowest gas emissivity and also the lowest T_{af} caused by higher concentration of CO_2. Case Air21 without the presence of particles had a q_{rad} lower than Case Oxy27W due to the lower gas emissivity. With particles, however, the case slightly exceeded the values of Case Oxy27W at particle flow rates over 100% of ash. This was because the inlet temperature (T_{af}) was higher and particles could emit more with higher radiation intensity.

The above results suggest that care must be taken when experimentally investigating the effect of FGR conditions on radiation. A pilot-scale furnace with a typical diameter of about 2 m or less with a single burner flame has been often used for experimental studies [4, 11]. Although the detailed profiles of radiation would vary by the properties of the flame, the average wall radiative heat flux measured at various combustion conditions may have different trends from those for commercial-scale boilers.

Fig. 6 compares the effect of WSGGMs under the presence of particles for Case Oxy27D. Note that the dry FGR case had the largest difference between the Smith model and the other two improved ones. With larger particle flow rates, the significant difference in q_{rad} gradually disappeared. This was due to the dominant effect of particles on radiation at high particle concentrations. At L_{mb}=8.31 m (Fig. 6(b)), the difference between WSGGMs was only 1.9 kW/m^2 (1.3%) when the particle flow rate was 100% of ash in the coal. In this case, the volume-averaged absorption coefficient of particles was 0.162 m^{-1} for L_{mb}=8.31 m, while that of gas was 0.080 m^{-1}. In Case Oxy27W, for comparison, the absorption coefficients were 0.217 m^{-1} for particles and 0.097 m^{-1} for gas. The values in Case Air21 were 0.172 m^{-1} and 0.065 m^{-1}, respectively. It implies that the effect of particle emission would be more significant in the other combustion cases. Therefore, the errors involved in the prediction of gas absorption coefficient became not critical for larger furnaces fired by pulverized coal.

Table 3. Key properties of product gas for air- and oxy-coal combustion with 24-30% of O_2 in the oxidizer.

Case		Air21	Oxy-coal combustion with wet FGR				Oxy-coal combustion with dry FGR			
			Oxy24W	Oxy26W	Oxy28W	Oxy30W	Oxy24D	Oxy26D	Oxy28D	Oxy30D
O_2 in the oxidizer (%)		21	24	26	28	30	24	26	28	30
Product gas	CO_2 (%)	12.80	47.48	47.36	47.24	47.12	77.48	76.27	75.08	73.92
	H_2O (%)	12.41	46.02	45.91	45.79	45.68	14.01	15.05	16.08	17.08
	P_w+P_c (atm)	0.252	0.935	0.933	0.930	0.928	0.915	0.913	0.912	0.910
	P_w/P_c	0.969	0.969	0.969	0.969	0.969	0.181	0.197	0.214	0.231
T_{af} (K)		2076	1885	1988	2088	2186	1797	1899	1999	2097
Cp at 1500K (kJ/kg·K)		1.361	1.660	1.658	1.657	1.656	1.400	1.406	1.413	1.419

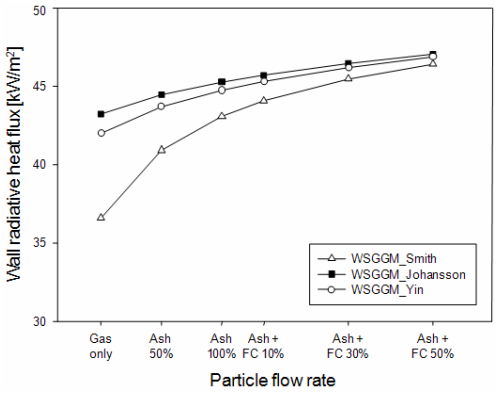

(a) L_{mb} = 1.66 m

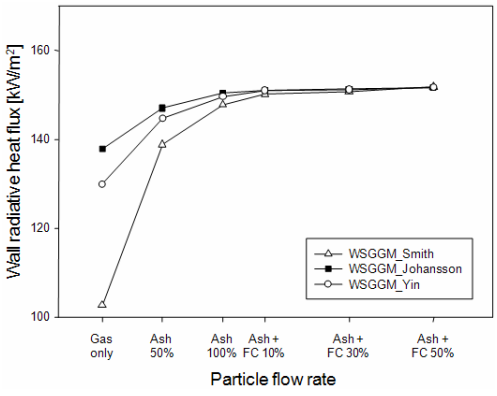

(b) L_{mb} = 8.31 m

Fig. 6. Effect of WSGGM for different particle flow rates on the average q_{rad} for oxy-fuel combustion with dry FGR condition (Case Oxy27D).

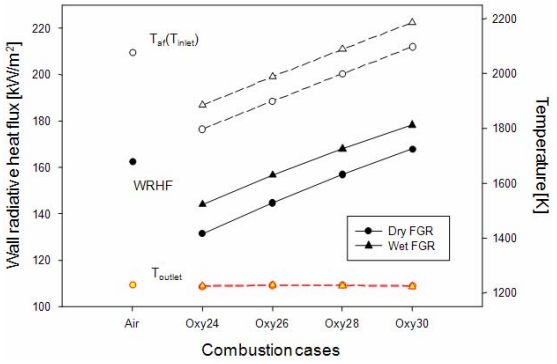

Fig. 7. Comparison of the average q_{rad}, T_{af} and outlet temperature for O_2 concentration of 24-30% in oxy-coal combustion (WSGGM: Yin model, L_{mb}=8.31m, particle: ash 100% + FC 10%).

4.5 Effect of O_2 concentration in the oxidizer

One of the critical parameters in the design of oxy-fuel furnace is the O_2 concentration in the oxidizer. It influences the flow rate, temperature and composition of combustion gas as well as the detailed flame characteristics. Based on the combustion calculation method in this study, the O_2 concentration in the oxidizer was varied from 24% to 30% for oxy-coal combustion with dry and wet FGR. Table 3 summarizes the key properties of product gas for the reference coal.

Fig. 7 compares the T_{af} and average q_{rad} for the cases with different O_2 concentration for oxy-coal combustion. The furnace size was 10 m×10 m×30 m (L_{mb} = 8.31 m) in these simulations. The particle flow rate was fixed at ash 100% and FC 10%. T_{af} and average q_{rad} increased proportionally to the O_2 concentration, and the values for the wet FGR cases maintained higher than the dry FGR ones. T_{af} for the oxy-coal combustion became similar to that of Case Air21 for O_2 concentration of about 28% for wet FGR and 30% for dry FGR. For q_{rad}, however, the oxy-coal case with wet FGR achieved a similar level when O_2 in the oxidizer was 27%. The dry FGR case required about 28.5% of O_2 due to the lower gas temperature. The distribution of heat flux in actual furnaces would vary depending on the characteristics of flames and furnace configuration (i.e., wall firing and tangential firing). Detailed assessment for the effect of O_2 concentration in the oxidizer on the flame shape, gas temperature and wall heat flux is an essential procedure in finalizing the boiler and furnace design of oxy-fuel combustion.

5. Conclusions

The wall radiative heat flux was numerically assessed for product gases representing oxy- and air-fuel combustion conditions in a simple hexahedral furnace. Three different WSGGMs were adopted for the calculation of radiation prop-

erties in the DO method. The key findings are as follows:

- Without presence of particles, the conventional Smith model significantly underestimated the gas emissivity and corresponding heat flux for oxy-fuel combustion. The largest error was found for the dry FGR conditions where the H_2O partial pressure became low.
- At a mean beam length of 8.3 m, the participation of particles saturated the wall radiative heat flux. Therefore, the use of WSGGM optimized for oxy-fuel combustion did not significantly affect the accuracy of radiation calculation for larger furnaces. For small furnaces with a mean beam length of a few meters, however, the accurate prediction of gas emission was still crucial.
- Oxy-coal combustion with dry FGR had lower values of q_{rad} than wet FGR, since the larger concentration of CO_2 in the product gas led to lower gas emissivity and T_{af}.
- O_2 concentration in the oxidizer was a key control parameter for oxy-fuel combustion, since its value directly influenced T_{af} and q_{rad}. In this simplified approach, the O_2 concentration to achieve the q_{rad} of air-fuel combustion was 27% for oxy-coal combustion with wet FGR and 28.5% for dry FGR. Further investigation is required for the effect of combustion characteristics in actual furnaces, such as the shape of flames and gas temperatures.

Acknowledgment

This study was supported by the Energy Efficiency & Resources Program of the Korea Institute of Energy Technology Evaluation and Planning (KETEP) grant (No. 2010201010108A) funded by the Korea government Ministry of Knowledge Economy.

Nomenclature

A : Wall surface area (m^2)
ASU : Air separation unit
DO : Discrete ordinate
E : Emission of particles
FC : Fixed carbon
FGR : Flue gas recirculation
I : Radiation intensity, total number of gray gases
J : Highest order of polynomial
L_{mb} : Mean beam length (m)
P : Partial pressure of H_2O and CO_2 (atm)
T : Temperature (K)
V : Furnace volume (m^3)
a : Weighting factor
c : Polynomial coefficient
f : Scattering factor of particles
j : Order of polynomial
q_{rad} : Radiative heat flux on the wall (kW/m^2)
r : Position vector
n : Refractive index
s, s : Direction vector, scattering direction vector

Greek

Φ : Phase function
Ω : Solid angle
α : Absorption coefficient (m^{-1})
ε : Emissivity
κ : Coefficient for absorption coefficient
σ : Scattering factor

Subscript

af : Adiabatic flame temperature
c : CO_2
i : Gray gas component
g : Gas
mw : Membrane wall
n : Projected
p : Particle
w : H_2O

References

[1] B. J. P. Buhre, L. K. Elliott, C. D. Sheng, R. P. Gupta and T. F. Wall, Oxy-fuel combustion technology for coal-fired power generation, *Prog. Energy Comb. Sci.,* 31 (2005) 283-307.

[2] T. Wall, Y. Liu, C. Spero, L. Elliott, S. Khare and R. Rathnam et al., An overview on oxyfuel coal combustion – State of the art research and technology development, *Chem. Eng. Res. Des.*, 87 (2009) 1003-1016.

[3] S. P. Khare, T. F. Wall, A. Z. Farida, Y. Liu, B. Moghtaderi and R. P. Gupta, Factors influencing the ignition of flames from air-fired swirl pf burners retrofitted to oxy-fuel, *Fuel*, 87 (2008) 1042-1049.

[4] S. Hjärtstam, K. Andersson, F. Johnsson and B. Leckner, Combustion characteristics of lignite-fired oxy-fuel flames, *Fuel*, 88 (2009) 2216-2224.

[5] R. K. Rathnam, L. K. Elliott, T. F. Wall, Y. Liu and B. Moghtaderi, Differences in reactivity of pulverised coal in air (O_2/N_2) and oxy-fuel (O_2/CO_2) conditions, *Fuel Processing Tech.*, 90 (2009) 797-802.

[6] H. Cao, S. Sun, Y. Liu and T. F. Wall, Computational fluid dynamics modeling of NOx reduction mechanism in oxy-fuel combustion, *Energy Fuels*, 24 (2010) 131-135.

[7] S. A. Skeen, M. K. Benjamin and R. L. Axelbaum, Nitric oxide emissions during coal and coal/biomass combustion under air-fired and oxy-fuel conditions*, Energy Fuels*, 24 (2010) 4144-4152.

[8] S. I. Keel, J. H. Yun and S. A. Roh, *Behavior of SO_3 in oxy-PC combustion field*, Int. Symp. on Low Carbon & Renewable Energy Technology, Jeju, Korea, Nov. 15-18, 2010.

[9] R. Johansson, K. Andersson, B. Leckner and H. Thunman, Models for gaseous radiative heat transfer applied to oxy-fuel conditions in boilers, *Int. J. Heat Mass Transfer*, 53 (2010) 220-230.

[10] C. Yin, L. C. R. Johansen, L. A. Rosendahl and S. K. Kær, New weighted sum of gray gases model applicable to computational fluid dynamics (CFD) modeling of oxy-fuel combustion: derivation, validation, and implementation, *Energy Fuels*, 24 (2010) 6274-6282.

[11] K. Andersson, R. Johansson, F. Johnsson and B. Leckner, Radiation intensity of propane-fired oxy-fuel flames: implications for soot formation, *Energy Fuels*, 22 (2008) 1535-1541.

[12] G. Krishnamoorthy, M. Sami, S. Orsino, A. Perera, M. Shahnam and E. D. Huckaby, Radiation modeling in oxy-fuel combustion scenarios, *Int. J. Comp. Fluid Dynamics*, 24 (3-4) (2010) 69-82.

[13] P. Edge, M. Gharebaghi, R. Irons, R. Porter, R. T. J. Porter, M. Pourkashanian, D. Smith, P. Stephenson and A. Williams, Combustion modelling opportunities and challenges for oxy-coal carbon capture technology, *Chem. Eng. Res. Des.*, 89 (9) (2011) 1470-1493.

[14] R. Siegel and J. R. Howell, *Thermal radiation heat transfer, 3rd ed., Hemisphere Publishing Corporation*, Washington, USA (1992).

[15] H. C. Hottel and A. F. Sarofim, *Radiative Transfer*, McGraw-Hill, New York (1967).

[16] T. F. Smith, Z. F. Shen and J. N. Friedman, Evaluation of coefficients for the weighted sum of gray gases model, *J. Heat Transfer*, 104 (1982) 602–608.

[17] Fluent Inc., *Fluent 6.3 user's guide*, Lebanon, New Hampshire, USA (2006).

[18] A. Willams, M. Pourkashanian and J. M. Jones, *Combustion and gasification of coal*, Tayor & Francis, New York (2000) 28.

[19] P. Basu, C. Kefa and L. Jestin, *Boilers and Burners: Design and Theory*, Springer-Verlag, New York, USA (2000) 132.

[20] J. Hong, J.A. Kim, C. Ryu and Y. Kim, Evaluation of operational characteristics in a 500 MWe opposed-fired coal boiler using computational fluid dynamics, *Proc. of 43th Symposium of Korea Society of Combustion*, Gyeongju, Korea (2011) 447-450.

Changkook Ryu is an associate professor in School of Mechanical Engineering at Sungkyunkwan University, Korea. He received his Ph.D degree on Mechanical Engineering at Korea Advanced Institute of Science and Technology (KAIST), in 2001. He was a research associate in Department of Chemical and Process Engineering at University of Sheffield, UK from 2002 to 2007. His research interests include energy conversion of biomass, coal and other fuels by combustion, gasification and pyrolysis.

Sanghyun Park received his B.S degree on Mechanical Engineering at Sungkyunkwan University, Korea. He is currently M.S. candidate in SKKU, Korea. His research interests are oxy-fuel combustion for CCS and pulverized coal combustion.